C. WAN[1]*, X. LI[1], H. XING[1]

COPPER CORROSION INHIBITION BY A QUATERNARY AMMONIUM SALT-ASSISTED BENZOTRIAZOLE

Quaternary ammonium salt (QAS) Hyamine 1622 and benzotriazole (BTAH) were used to form a protective layer on copper surface to resist the corrosion by immersing the copper into the inhibitors-containing solutions. The inhibitor's anticorrosion properties are studied in neutral 3.5 wt.% NaCl medium by anodic polarization, Tafel polarization, electrochemical impedance spectroscopy (EIS) and OCP exposure. The surface characterization is analyzed by Contact angle(CA) measurement, X-ray photo-electron spectroscopy (XPS), and scanning electron microscopy(SEM). The electrochemical tests show that they can act as single inhibitor to form a passive layer to resist Cu corrosion, and the anticorrosion properties of Cu can be improved by using binary Hyamine 1622/BTAH inhibitors. XPS results indicate that both BATH and Hyamine 1622 molecule can be chemisorbed onto the copper surface and make complex films with Cu species. CA measurement revealed the enhancement of hydrophobicity by combining QSA with BTAH. OCP exposure in neutral medium for 72 h evidently reveals that the passive layer formed by binary inhibitors decreases the pit corrosion. Better hydrophobic nature and more compact passive layer give rise to excellent inhibition properties of binary inhibitors.

Keywords: Copper anticorrosion; Quaternary ammonium salt; Benzotriazole

1. Introduction

Copper and its alloys are important metals that are widely applied in electronics, mechanics, and facilities due to their excellent electrical and thermal conductivity, electromigration resistance, mechanical properties, and stability. They can be designed as wires, sheets, pipelines, and nanoparticles for various applications, such as current collectors, heat exchanges system, catalysts, antimicrobial agents etc. [1-6]. Copper mass is resistant toward the attack of the atmosphere and many chemicals; however, it is well prone to corrosion by oxygen or the aggressive species when it is exposed to moisture or chloride/sulphate-containing solution [4]. In its practical use, its varnish and the reduction of its conductivity often happen. Therefore, keeping the stable performances of copper becomes important in the application of copper materials. In recent years, establishing protective films on the metal surface has become one of the most effective methods to maintain the basic properties of metal, delay metal corrosion and protect the metal from corrosive ions [4,7]. Many film-forming techniques on the copper surface have been established to resist the corrosion, such as coating [8-10], electro-plating [11], nanocomposite film [12,13], and organic corrosion inhibitors [7,14-24]. Among these techniques, organic corrosion inhibition on copper surface is considered as one of the simplest and most effective means because of its ease of fabrication, efficiency, and the possibility of preparing monolayers [14-24]. So far, many organic compounds containing O, N, or S heteroatoms with or without π-system heterocyclic groups have been studied as effective copper inhibitors, and they are able to adsorb on the surface to form a compact film that will suppress the corrosion process [15-18,23].

Benzotriazole (BTAH) possessing benzene and triazole rings (see Fig. 1a) is popular copper corrosion inhibitor for its high efficiency in various media, including the atmosphere [18-24]. Many researchers report that the efficiency of BTAH is based on its adsorption on the copper surface and the formation of Cu(I)BTA barrier film, which has low solubility in aqueous media [20,21,24]. The Cu(I)BTA film can act as a physical barrier, hindering the diffusion of aggressive ions [20,25-27]. However, the corrosion inhibition efficiency of a single BTAH inhibitor is limited, and many works have been focused on the synergistic effect of different inhibitors or the new organic

[1] SHANGHAI INSTITUTE OF TECHNOLOGY, SCHOOL OF CHEMICAL AND ENVIRONMENTAL ENGINEERING, SHANGHAI, 201418

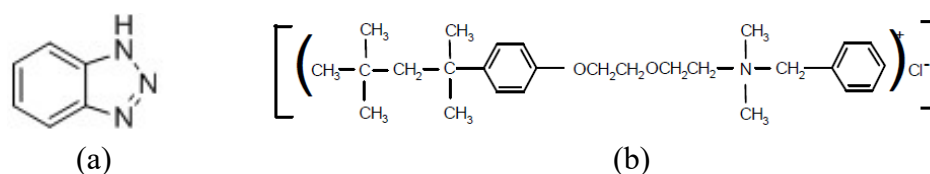* Corresponding author: cywan@sit.edu.cn

Fig. 1. Chemical structure of (a) BTAH and (b) QAS Hyamine 1622

inhibitor as alternatives [13,15-18,21,22,25,28,29]. Quaternary ammonium compounds (QACs) are cationic surfactants where alkyl or aryl groups (*i.e.* benzyl groups) replace ammonium hydrogen to create strong base and corresponding salts. Their ability to disrupt microorganism lipid membranes makes them the commercial disinfectant [30,31]. As Cationic surfactants, the hydrophilic portion contains a positively-charged ammonium cation which is readily adsorbed on the negative-charged surface, and an alkyl chain of various lengths comprises the hydrophobic portion which is repelled to water. Hence, QACs are also studied as metal corrosion inhibitor [32,33] or the additive for metal electrodeposition [34]. Quaternary ammonium salt (QAS), Hyamine 1622 (chemical structure shown in Fig. 1a) is a water soluble cationic surfactant and widely used as a bactericide because of its high germicidal activity in hard water. It contains aromatic rings with delocalized π electrons, high molecular weight alkyl chains, and N heteroatom with free electron pairs, that are favorable to anticorrosion of metal [7]. Hence, it is also expected to be used as a metal corrosion inhibitor for its compatibility with nonionic surface active agents and most polar solvents.

In the present work, BTAH and QAS, Hyamine 1622 are applied to form inhibition film on the copper surface by self-assembling in containing single or binary solution. The inhibition effects of BTAH and Hyamine 1622 on copper corrosion in 3.5% NaCl solution are studied.

2. Experimental

2.1. Materials

The BTAH and Hyamine 1622 were supplied by Sinopharm Chemical Reagent Co., Ltd. and Hozen International Trading (Shanghai) Co., Ltd., respectively. BTAH was dissolved in distilled water to prepare a 3 g L^{-1} solution. Hyamine 1622 was dissolved in a 3 g L^{-1} BTAH solution to prepare solutions containing 0.2-2 g L^{-1} Hyamine 1622. The copper specimens (purity: 99.99%) were used as the working electrodes. Before use, the copper surface was sequentially polished with different metallographic grits paper and then cleaned in dilute ethanol for a few minutes, followed by drying with a flow of nitrogen gas. The cleaned electrodes were directly put in different solutions to assemble inhibitor films at 40°C. After 10 minutes, the assembled samples were taken out of the solutions and washed several times with distilled water to remove the solution residue. The cleared assembled copper samples were used for electrochemical measurements and characterization.

2.2. Electrochemical characterization

Electrochemical measurements to investigate the corrosion protection performance of the inhibitor layer were carried out in 3.5 wt.% NaCl solution by Gamry electrochemical workstation (Reference 600+, America). All experiments were carried out using a conventional three-electrode system consisting of the Cu/filmed Cu electrode as working electrode, platinum electrode as counter electrode, and saturated calomel electrode (SCE) as reference electrode. Potentiodynamic polarization was scanned in the potential range of –250 mV to +250 mV (vs. OCP) at a scan rate of 1 mV s^{-1}. The inhibition efficiency can be evaluated using the corrosion current density as follows:

$$IE\,(\%) = \frac{i^0_{corr} - i_{corr}}{i^0_{corr}} \times 100 \qquad (1)$$

where i^0_{corr} and i_{corr} are the corrosion current densities of the bare and inhibitor modified electrodes, respectively. The electrochemical impedance spectroscopy (EIS) measurement was carried out at amplitude potential perturbation of 10 mV in the AC frequency range from 100 kHz to 0.1 Hz. The obtained impedance results were analyzed and fitted by ZSimpWin 3.2.1 impedance analysis software. The inhibition efficiency can be measured using the charge transfer resistance from the following equation:

$$IE\,(\%) = \frac{R'_{ct} - R_{ct}}{R'_{ct}} \times 100 \qquad (2)$$

where R'_{ct} and R_{ct} are the charge transfer resistance for the inhibitors coated Cu and bare Cu, respectively. The OCP of bare Cu and inhibitors coated Cu was monitored in 3.5 wt.% NaCl solution under static. All the electrochemical experiments were carried out at room temperature.

2.3. Physical characterization

A goniometer coupled with CAM software (Shanghai Zhongchen Digital Technic Apparatus Co. Ltd) was used to measure the contact angle of a DIW drop placed on the surfaces of the bare Cu and the Cu surface immersed in the solutions containing BTAH, Hyamine 1622 or their combination. The data were obtained from three different samples, and the average numbers are reported. Scanning electron microscopy (SEM; FEI Nova NanoSEM × 30) was used to observe the morphology of Cu surface after static exposure in 3.5 wt.% NaCl solution for 72 h to compare anticorrosion ability for different inhibitors.

3. Results and discussion

3.1. Time evolution of corrosion potential

The clean bare coppers are immersed in an inhibitor-containing solution at 40°C for 10 minutes to form a film on the copper surface. In order to determine the effects of the films on the corrosion potential of copper, the free dissolution of bare Cu and the filmed Cu surface were monitored, and the open circuit (corrosion) potentials (E_{corr}) with respect to time were recorded. Fig. 2 shows typical mean open circuit (corrosion) potential (E_{corr}) transients for Cu electrodes containing different inhibitor layers in a 3.5 wt.% NaCl solution at room temperature. Compared to the bare Cu electrode, all the E_{corr} values of the filmed Cu electrodes shift to a positive direction, indicating a resistance of the anodic corrosion reaction of copper. With the increase of the immersing time in NaCl solution, the E_{corr} of Cu electrode containing BTAH inhibitor decreases greatly, indicating that the BTA film is destroyed by aggressive Cl$^-$ or Cl$^-$ species immigrating to the copper surface through the holes of BTA films. The E_{corr} of Cu electrode treated on 1 g L^{-1} Hyamine 1622 is reasonably stable with the increase of immersion time, indicating the stability of the Hyamine 1622 film. The great E_{corr} increase happens when the combination of BTAH and Hyamine 1622 is carried out, and no obvious decrease occurs with the increase of immersion time in NaCl solution, indicating that the obtained film is compact and stable on the copper surface and has an increased resistance of corrosive species to the copper surface. Hence, in the presence of Hyamine 1622, the surface of copper can be more protected by binary inhibitors from corrosion.
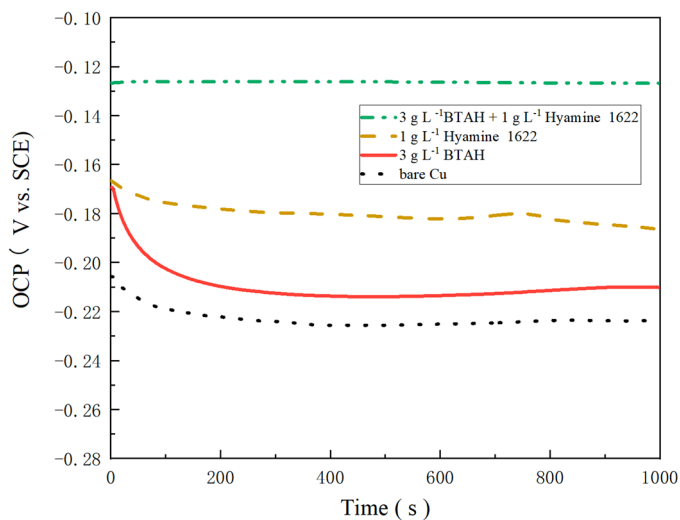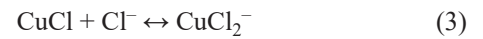

Fig. 2. potential vs. time curves in 3.5 wt.% NaCl for the bare Cu and the inhibitor coated Cu surface

3.2. Potentiodynamic polarization study

Many researches have reported that the corrosion mechanism of copper is strongly effected by chloride ions, and the presence of surface films formed on copper evidently reduces the rate of both anodic and cathodic charge transfer process [7,35]. The effect of different films on copper corrosion was investigated by the polarization technique. Typical anodic polarization behaviors of bare Cu and inhibitor filmed Cu are shown in Fig. 3. The anodic behavior of bare Cu can be explained using the following reactions [7,13, 35].

$$Cu^0 - e \rightarrow Cu^+ \qquad (1)$$

$$Cu^+ + Cl^- \rightarrow CuCl \qquad (2)$$

$$CuCl + Cl^- \leftrightarrow CuCl_2^- \qquad (3)$$

$$Cu^+ - e \rightarrow Cu^{2+} \qquad (4)$$

In neutral chloride solution, the first step is the oxidation of Cu^0 to Cu$^+$ (reaction 1), and Cu$^+$ ions rapidly react with Cl$^-$ to produce CuCl which is only slightly soluble in dilute chloride solution (reaction 2). The insoluble CuCl film will cover the surface of copper. The rate of Cu$^+$ production and the current density increase with the positive shift of overpotential. However, Cl$^-$ can attack CuCl and produce soluble CuCl$_2^-$ (reaction 3). Hence, at an overpotential region, when the production rate of Cu$^+$ is larger than the consumption rate, a peak value of current density appears (the peak I shown in Fig. 3), indicating a passive film formation. The increase of subsequent current density with the increase of anodic overpotential is due to the CuCl$_2^-$ production and Cu^{2+} formation (reaction 4), which usually exist in the form of Cu(OH)$_2$, Cu$_2$(OH)$_3$Cl or CuCO$_3$.Cu(OH)$_2$ [7]. Evidently, compared to the bare Cu electrode, the inhibitor-filmed Cu has a reduced dissolution rate, indicating that a single inhibitor (BATH or QSA Hyamine 1622) can react with Cu and form a passive barrier to resist Cu corrosion. For BATH, similar to bare Cu, evident passivation occurs, indicating the inhibitor layer with BATH is not so compact that aggressive species can penetrate through the hole to make copper dissolution and CuCl formation. Tiny peak I for Hyamine 1622 inhibitor in its anodic
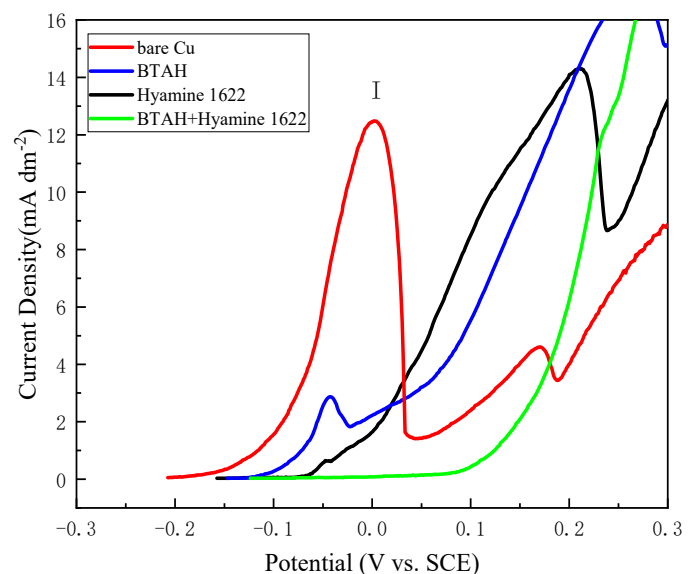

Fig. 3. Typical anodic polarization behaviors of bare Cu and inhibitor filmed Cu in 3.5 wt.% NaCl solution

polarization curve reveals that a compact film is formed when Cu is immersed in 1 g L^{-1} Hyamine 1622 for 10 minutes. The layer obtained from binary inhibitors shows an excellent barrier property and no evident anodic reaction of Cu in the initial anodic polarization potential region, indicating the combination of BATH and Hyamine 1622 can produce a compact film on copper to separate Cu from aggressive species in solution and reduce copper corrosion.

In order to compare the corrosion current density for different filmed copper treated by different inhibitors, the potentiodynamic polarization curves of bare Cu electrode and Cu electrodes covered different inhibitor layers in 3.5 wt.% NaCl solution were recorded with the sweep rate of 1 mV s^{-1} and shown in Fig. 4. It is obvious that all the cathodic portions in polarization curves are similar, and the anodic portion changes with the different Cu surfaces. For the bare copper electrode, the corrosion current density decreases when the polarization potential increases up to 0.1 V vs. SCE and then increases when the polarization potential shifts positive enough. The decrease of corrosion current density is mainly caused by the formation of the cuprous chloride as a result of the reaction in Eq. (1) [7,13]. Cuprous chloride is poor soluble in dilute NaCl solution and can produce a passive film on the copper surface to inhibit the copper corrosion for its resistance of charge transfer and mass transportation [7]. Compared to the bare Cu electrode, all coated copper electrodes have decreased cathodic current density and anodic current density, indicating the positive effect of corrosion inhibition for copper. When copper is treated in 1 g L^{-1} Hyamine 1622 solution, no obvious anodic passivation occurs at the anodic polarization region. But the increase of corrosion current density slows down at the anodic polarization potential which is not very far away from the corrosion potential. This may be due to the adsorption of Hyamine 1622 on the Cu surface and forming a compact inhibitor layer, which resists the Cu dissolution. The BTAH can greatly decrease the corrosion current density , and a passive film is formed on the Cu surface at around –0.03 V vs. SCE, which is more negative than that of the bare Cu electrode (appropriately 0.04 V vs. SCE). The negative shift of passivation potential and the decrease of current density are mainly caused by the formation of Cu(I)BTA film as a physical barrier, disabling the diffusion of aggressive ions [18,38]. When Hyamine 1622 is combined with BATH, the values of both cathodic and anodic current density decrease with the increase of Hyamine 1622, indicating the combination of Hyamine 1622 with BATH can suppress the active Cu dissolution. With the increase of Hyamine 1622, the similar anodic passive potential and the weakened passivation phenomenon indicate that enough QAS Hyamine 1622 improves the compatibility of the inhibitor layer and decrease the Cu dissolution. The calculated values of the polarization data according to Fig. 4 are presented in TABLE 1. It can be seen that the values of E_{corr} shift between the blank and inhibited curves are less than 85 mV, indicating the inhibitors act as mixed-type inhibitors and affect both the anodic and cathodic processes [39,40]. A limited corrosion inhibition ability for BTAH or Hyamine 1622 indicates their film on copper surface can resist the Cu dissolution to some extent. When Hyamine 1622 is combined with BATH, The content increase of Hyamine 1622 can reduce both cathodic and anodic corrosion current densities. The percentage inhibition efficiency (*IE* %) increases concurrently with an increase in the concentration of Hyamine 1622 in 3 g L^{-1} BTAH solution. The highest percentage inhibition efficiency value was achieved at the combination of 1.0 g L^{-1} Hyamine 1622 with 3.0 g L^{-1} BTAH. The increase of corrosion inhibition for binary inhibitors reveals that there is a more impact film obtained in binary inhibitor solution which can act as a physical barrier to protect the copper from dissolution.
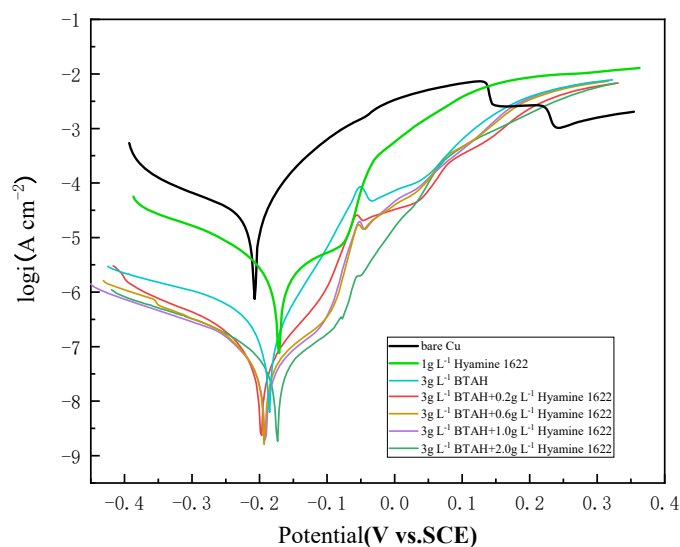

Fig. 4. Potentiodynamic polarization curves of bare Cu electrode and Cu obtained in solutions containing different inhibitors

TABLE1

Polarization parameters for bare Cu and different inhibitor-coated Cu in 3.5 wt.% NaCl solution

Concentrations	E_{corr} (mV vs. SCE)	i_{corr} (μA cm^{-2})	*IE* (%)
Bare Cu	–206	32	
3 g L^{-1} BTAH	–183	0.78	97.56
1 g L^{-1} Hyamine 1622	–172	2.54	92.07
3 g L^{-1} BTAH + 0.2 g L^{-1} Hyamine 1622	–197	0.041	99.87
3 g L^{-1} BTAH+ 0.6 g L^{-1} Hyamine 1622	–193	0.037	99.88
3 g L^{-1} BTAH + 1 g L^{-1} Hyamine 1622	–192	0.032	99.99
3 g L^{-1} BTAH + 2 g L^{-1} Hyamine 1622	–175	0.062	99.81

3.3. EIS studies

A film will be formed on the cupper surface when the cupper electrode is immersed in the solution containing BTAH or Hyamine 1622 by self-assembly [21,32]. The corrosion inhibition ability of the inhibitor for a metal can also be evaluated by

EIS which is one of the most helpful technique for the corrosion determination of coated metals. Fig. 5 shows the Nyquist impedance plots in 3.5 wt.% NaCl solution for the bare Cu and the Cu electrodes modified in different solutions. Compared to BATH and the combination of BATH and Hyamine 1622, the Nyquist spectra of the bare copper electrode and the Hyamine 1622 alone in 3.5 wt.% NaCl solution display poorly resolved loops. The figure inserted in Fig. 5a shows that there are two capacitive loops for bare Cu and the loop increases when the copper is treated in 1 g L^{-1} Hyamine 1622. It indicates that a film is formed on Cu surface in 1 g L^{-1} Hyamine 1622 solution and has a larger impedance. When Cu is put in BATH-containing solution, the Cu electrode has a resolved loop at high frequency followed by Warburg impedance at low frequency, indicating a reasonably large impedance. When Hyamine 1622 is combined with BATH, an enlarged loop appears, and the Warburg impedance disappears at low frequency with the increase of the concentration of Hyamine 1622. This indicates a more compact inhibitor film is formed on the Cu surface, which inhibits the corrosion process

at the interface of Cu and solution, and the corrosion process is mainly controlled by the charge transfer process while the corrosion resistance of copper has been enhanced significantly by the combination of BTAH and Hyamine 1622 [13,36]. Fig. 5b depicts the Bode plots of (φ vs. log f and log $|Z|$ vs. log f) bare electrode and inhibitor modified Cu electrodes. There is an increase in the value of the bode modulus and the bode phase angles for the modified electrodes, indicating the corrosion resistivity of Cu electrode by inhibitors layer. The combination of Hyamine 1622 and BATH enhances the corrosion resistivity of inhibitor film, and thelargest protection occurs when 1 g L^{-1} Hyamine 1622 is combined with 3 g L^{-1} BATH. Excessive Hyamine 1622 doesn't give evident enhancement on Cu anticorrosion in neutral solution.

In order to understand the electrochemical performance of the film on copper, the impedance data is elucidated using the equivalent circuit shown in Fig. 5b [13]. The electrochemical element R_s represents the resistance of the solution between the working electrode and the reference electrode. Its value can be
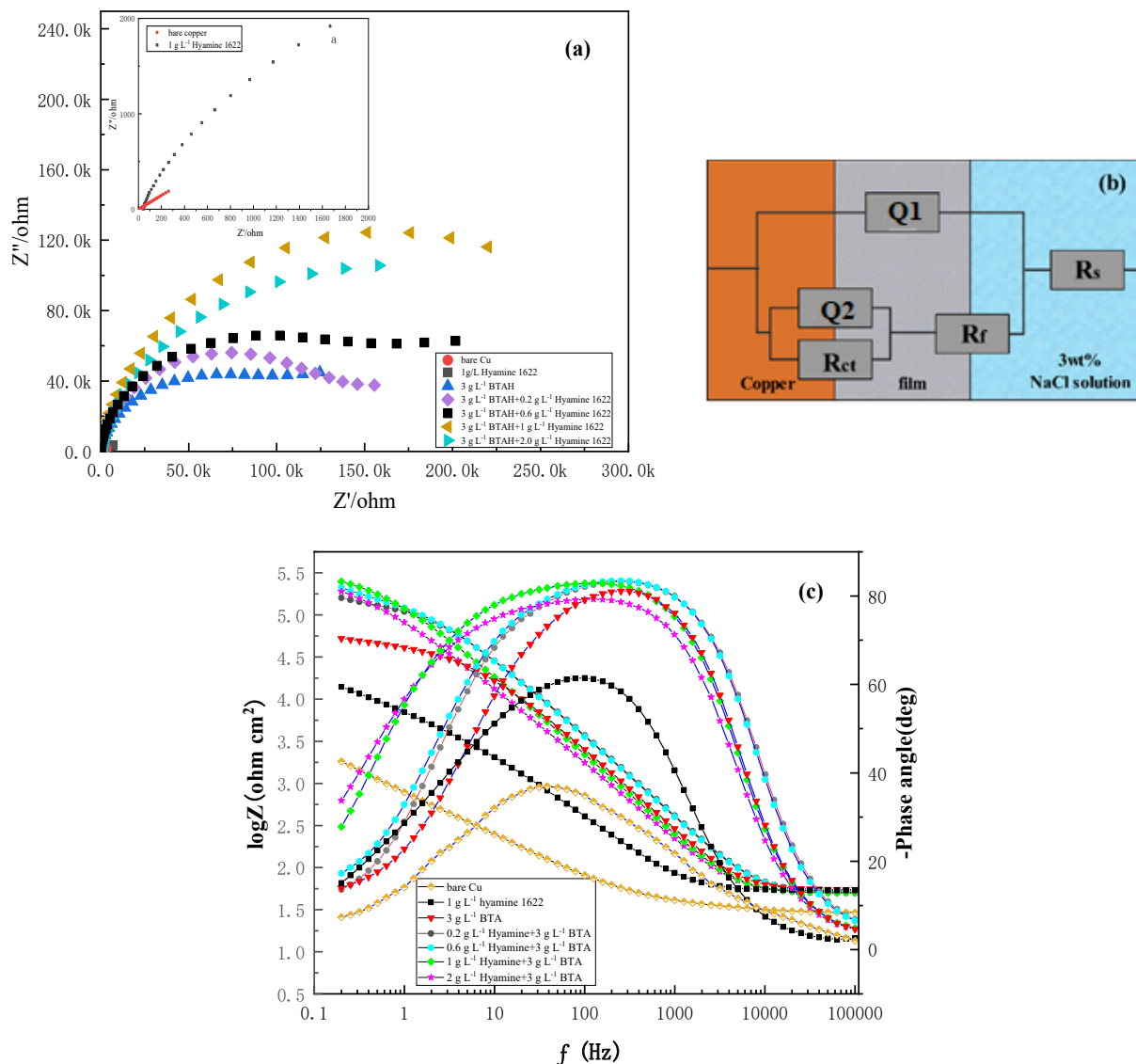

Fig. 5. (a) Nyquist plots in 3.5 wt.% NaCl for bare Cu and SAMs-coated Cu electrodes, (b) Equivalent circuit model to fit EIS experiment data, (c) Bode-Phase angle plots in 3.5 wt.% NaCl for bare Cu and SAMs-coated Cu electrodes

calculated from the intercept of the high-frequency semicircle with the real imagine axis. Constant phase element (Q1) typically represents the displacement of a pure double-layer capacitor [37], which is composed of a film capacitance C_f of the corrosion process and the deviation parameter n_1. The capacitance C_f mainly originates from the dielectric property of surface film formed on the copper surface (corrosion products and/or inhibitor film), and R_f represents the resistance of the film. R_{ct} is related to the charge transfer resistance of the corrosion process, and Constant Phase Element Q_2 is composed of double-layer capacitance and a dispersion coefficient n_2. The coefficient n can characterize different physical phenomena like surface inhomogeneity resulting from surface roughness, impurities, inhibitor adsorption, porous layer formation etc. The physical parameters of the EIS analysis obtained by the fitted equivalent circuit (Fig. 5b) are listed in TABLE 2. It shows that the film resistance R_f for BATH is lower than that of Hyamine 1622, indicating that the positively-charged ammonium cation is adsorbed and forms a high resistant film on the copper surface. The higher capacitance C_f and lower n_1 indicate that the film formed by Hyamine 1622 is less compact than BATH. According to equation (2), the corrosion resistance efficiency can be calculated from the change of electron transfer resistance between the bare copper electrode and the inhibitors-coated electrode. The copper corrosion resistance efficiency (IE%) is 98.04% for BATH-assembled copper and 93.27% for Hyamine 1622 treated copper. When Hyamine 1622 is combined with BATH, the obtained film has a larger R_{ct}, and its value increases gradually with the increase of the concentration of Hyamine 1622 in 3 g L^{-1} BATH solution, indicating the increase of corrosion resistance ability. The highest copper corrosion resistance efficiency of 99.54% is obtained when 1 g L^{-1} Hyamine 1622 is combined with 3 g L^{-1} BATH. The decrease of capacitance and n for the SAMs films from the combined inhibitors indicates that Hyamine 1622 can decrease the porosity and the surface heterogeneity due to the accumulation of inhibitor molecules on the most active adsorption sites [41]. When the concentration of Hyamine 1622 is above 1 g L^{-1}, the obtained film doesn't produce a great increase in copper corrosion inhibition efficiency. This result indicates a limiting action for the absorption of BATH and Hyamine 1622 on the copper surface, and too much Hyamine 1622 formula may affect the effective absorption of BTAH on the copper surface.

3.4. Inhibition mechanism study

Evidently, a blocking barrier is established when the copper surface is immersed in a solution containing BTAH, Hyamine 1622, or their combination. Considering the molecular structure of these organic compound, the contact angles of a DIW drop on the surface of bare Cu and filmed Cu samples that are immersed in 3 g L^{-1} BTAH, 1 g L^{-1} Hyamine 1622, and their combined solution are shown in Fig. 6. The contact angles of Cu samples exposed to BTAH solution is 76±2° while the contact angles of Cu samples exposed to Hyamine 1622 solution is 79±2°. The Combination of BTAH and Hyamine 1622 increases contact angle to 85±2°. Compared to the bare copper surface, all filmed Cu surfaces show a significant increase in contact angles, indicating the hydrophobic increase of Cu surfaces because the blocking film is formed by the reaction of Cu with BTAH or Hyamine 1622. BTA contains N atoms in its aromatic ring, and the benzene rings of adsorbed BTA molecules face away from Cu and make it hydrophobic [7,42]. Aromatic rings and high molecular weight alkyl chains in Hyamine 1622 also enhance the hydrophobicity of the copper surface. The fact that the combination of Hyamine 1622 and BTAH enhances the hydrophobicity of Cu surface shows that there is a positive effect of Hyamine 1622 on the barrier formation of BTAH for copper anticorrosion.
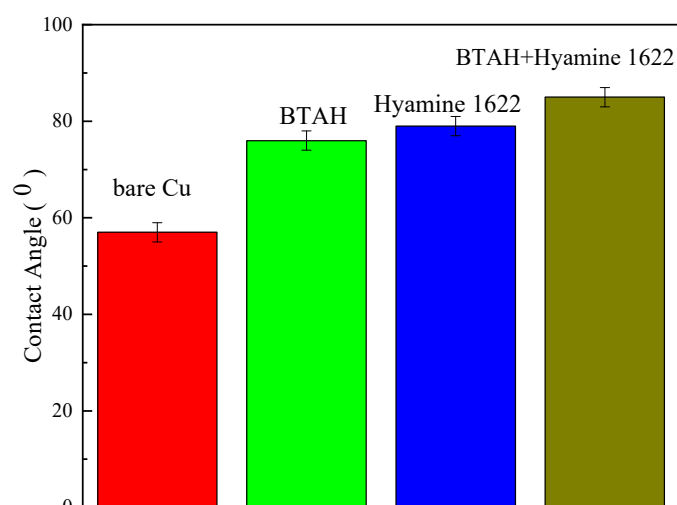

Fig. 6. Contact angles measurements of a DIW drop on bare Cu and filmed Cu surfaces that were immersed in different solutions

TABLE 2

EIS parameters obtained in 3.5 wt.% NaCl for the bare and Cu electrodes modified in different inhibitor-containing solution

Concentrations	Q_1		R_f (Ω cm^2)	Q_2		R_{ct} (kΩ cm^2)	IE%
	C_f (μF.cm^{-2})	n_1		C_{dl} (μF.cm^{-2})	n_2		
Bare Cu	—	—	—	104	0.54	1.58	—
3 g L^{-1} BTAH	0.86	0.979	2.40	9.13	0.46	56.23	97.19
1 g L^{-1} Hyamine 1622	18.7	0.877	38.2	16.64	0.45	23.48	93.27
3 g L^{-1}BTAH + 0.2 g L^{-1} Hyamine 1622	0.638	0.954	4.71	4.82	0.59	82.88	98.09
3 g L^{-1}BTAH+ 0.6 g L^{-1} Hyamine 1622	0.685	0.978	25.17	3.87	0.63	107.81	98.53
3 g L^{-1}BTAH + 1 g L^{-1} Hyamine 1622	0.782	0.977	23.23	3.23	0.62	344.79	99.54
3 g L^{-1}BTAH + 2 g L^{-1} Hyamine 1622	1.63	0.948	38.42	4.86	0.60	297.71	99.47

XPS was performed to verify the composition of the inhibitor layer on the Cu surface. XPS high resolution spectra for Cu surfaces treated with different inhibitors are shown in Fig. 7. Sample "a" is the as-received Cu surface immersed in 3 g L^{-1} BTAH solution at 40°C for 10 min. Sample "b" and "c" were the Cu surfaces immersed in solutions containing 1 g L^{-1} QAC Hyamine 1622 and the mixture of 3 g L^{-1} BTAH and 1 g L^{-1} QAC Hyamine 1622 at 40°C for 10 min, respectively. The high resolution spectra of Cu $2p_{3/2}$ from sample "a", "b" and "c" are shown in Fig. 7a. The three components of Cu $2p_{3/2}$ for sample "a" indicate the layer obtained from BATH contains metallic Cu at 932.7 eV [43,44], Cu_2O at 932.4 eV [16,43], and the Cu-BTA organometallic complex at 933.3 eV [16,29]. The Cu $2p_{3/2}$ spectrum of sample "b" is similar to that of sample "a", indicating QAC Hyamine 1622 can also be adsorbed on the Cu surface and form a layer with Cu. The high resolution N 1s spectra of three samples are illustrated in Fig. 7b. the N1s bond energy of BATH emerges at 399.3 eV [43]. For sample b, there are two peaks for N 1s signal in high resolution spectrum. The bond energy at 403.11 eV is attributed to the quaternary nitrogen (R_4^+) in the cation [45-47]. The N 1s signal at 398.7 eV is attributed to nitrogen of the amide groups and sp^2 hybridization [48] coming from amide traces present in the Hyamine 1622. Two bond energy peaks for N 1s for sample "c" can be observed as expected. One peak at 403.11 eV is from QAS Hyamine 1622 and the other at 399.4 eV is mainly from BTAH. The results of Cu 2p and N 1s for sample "c" indicate that the barrier layer consists of the Cu-BTA/Cu-QAS organometallic complex as well as Cu_2O. It is also interesting that the signal intensity of BATH for sample "c" is higher compared to that for sample "a", indicating QAS Hyamine 1622 enhances the adsorption of BATH on the Cu surface. It is well established in the literature that NR_4^+ can be adsorbed on Cu or Fe surfaces through Cl$^-$ as a bridge [49,50]. Hyamine 1622 is a kind of QAS containing chloride. Hence, a Cu-QAC passive film may be formed through Cl$^-$ as a bridge when Cu is immersed in a solution containing Hyamine 1622. The signal with BE = 197.6 eV (Cl 2p) assigned to Cl$^-$ ions in sample "b" and "c" confirms the function that RN_4^+ is adsorbed on the Cu surface and forms a passive layer with BTAH to inhibit Cu corrosion. The higher hydrophobicity and more compact BTA adsorption for the barrier layer of sample "c" is benefitial to Cu anticorrosion.

3.4. Surface morphology studies

In order to gain the surface morphological changes of Cu, copper surfaces with OCP exposure in 3.5 wt.% solutions for 72 h were evaluated by SEM, as shown in Fig. 8. After 72 h immersion in NaCl solution, the bare Cu surface became brown-black,
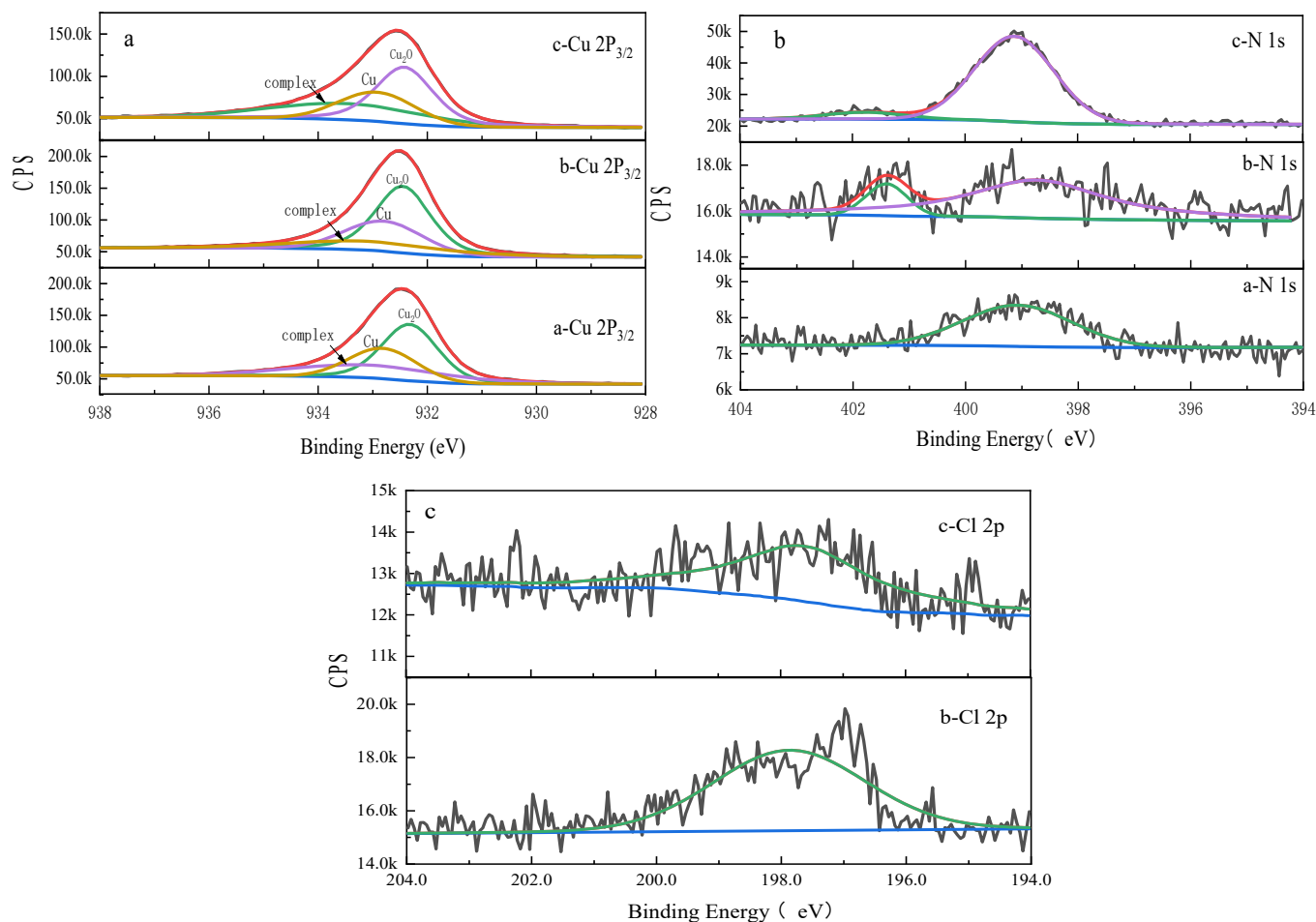

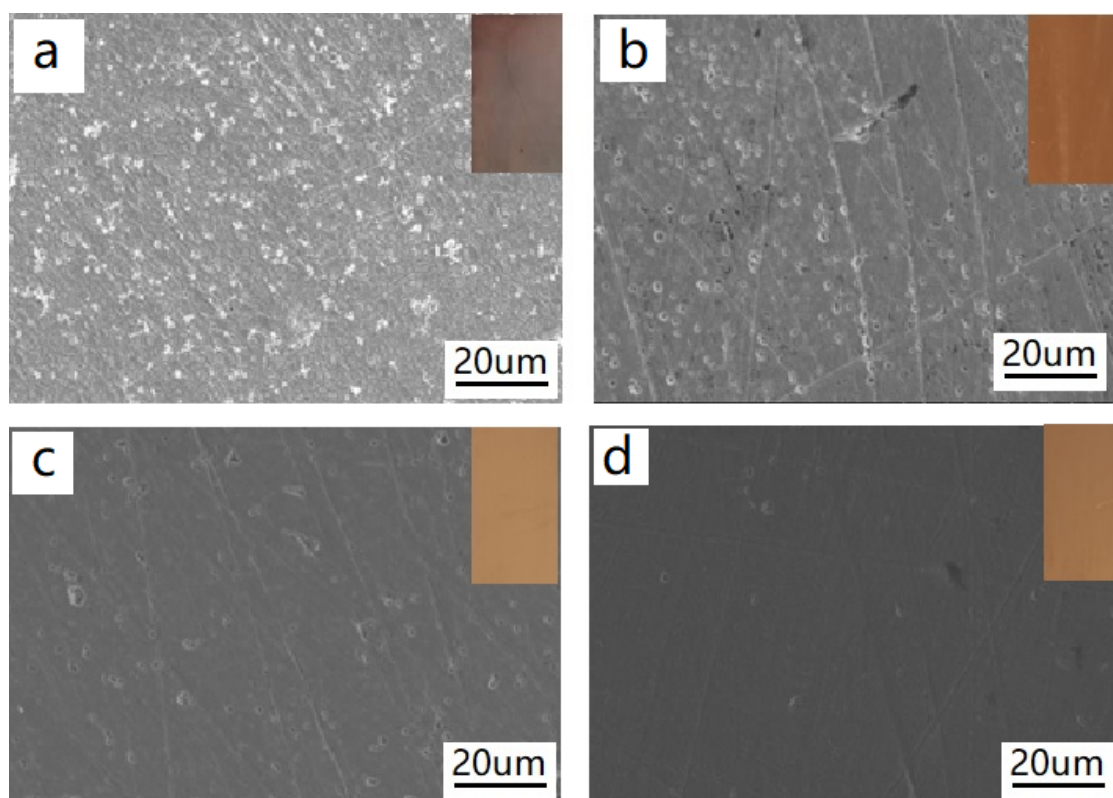Fig. 7. XPS high-resolution spectra of (a) Cu 2p, (b) N 1s and (c) Cl 2p from sample "a", "b" and "c"

Fig. 8. SEM micrographs of copper surfaces subsequent to 72 h OCP exposure in 3.5 wt.% NaCl solution. (a) bare Cu; (b) Cu treated in 3 g L^{-1} BTAH; (c) Cu treated in 1 g L^{-1} Hyamine 1622; (d) Cu treated in 3 g L^{-1} BTAH and 1 g L^{-1} Hyamine 1622

indicating that the copper surface has been eroded in the attack of aggressive species such as Cl^{-} and dissolved oxygen in solution. A lot of corrosion products are observed on the copper surface (Fig. 8a). When copper is coated with BATH or Hyamine 1622 inhibitors, the surface color changes mildly, and the SEM images (Fig. 8b and Fig. 8c) reveal that there are some pits on the copper surface. This indicates that the single inhibitor film is not compact enough, and aggressive species penetrate through the hole of the film and corrode Cu. Whereas in the presence of layer formed in the mixture of 1 g L^{-1} Hyamine 1622 and 3 g L^{-1} BATH, the morphology of Cu (Fig. 8d) looks relatively smooth with no noticeable corrosion, indicating the combination of Hyamine and BATH can effectively protect the Cu from corrosion in the aggressive environment.

4. Conclusions

In this work, BATH and QAS Hyamine 1622 were used to form a passive layer on the copper surface to improve anticorrosion properties, and the inhibition properties were studied in a neutral medium. Both BATH and Hyamine 1622 can act as inhibitors to form a passive layer as a physical barrier layer to resist Cu corrosion. The anticorrosion properties can be improved by using binary Hyamine 1622/BTAH inhibitors. The optimum concentration of BTAH and Hyamine 1622 on the surface has been established by potentiodynamic polarization and EIS methods. The surface characteristics of inhibitor coated Cu were characterized and compared by contact angel test and XPS. The results show that both BATH and Hyamine 1622 molecule can be chemisorbed onto the copper surface, and Hyamie 1622 improves the adsorption of BATH on copper and enhances the hydrophobicity and varnish of copper. The protection of inhibitors on Cu corrosion in 3.5 wt.% NaCl was investigated by anodic polarization, Tafel polarization, EIS, and OCP exposure for 72 h, showing excellent inhibition properties of binary inhibitors.

REFERENCES

[1] N. Vu, L. Daeho, Copper Nanowires and Their applications for flexible, transparent conducting films: A review, Nanomaterials **6**, 47-63 (2016).
DOI: https://doi.org/10.3390/nano6030047

[2] A. Mazloum-Nejadari, G. Khatibi, B. Czerny, M. Lederer; J. Nicolics, L. Weiss, Reliability of Cu wire bonds in microelectronic packages. Microelectronics Reliability, **74,** 147-154 (2017).
DOI: https://doi.org/10.1016/j.microel.2017.04.014

[3] A. Abbasa, S. Abbas, X.L. Wang, Nanoporous copper: fabrication techniques and advanced electrochemical applications, Corr. Rev. **34**, 249-276 (2016).
DOI: https://doi.org/10.1515/corrrev-2016-0023

[4] H. Bi, G.T. Burstein, B.B. Rodriguez, G. Kawaley, Some aspects of the role of inhibitors in the corrosion of copper in tap water as observed by cyclic voltammetry, Corro. Sci. **102**, 510-516 (2016).
DOI: https://doi.org/10.1016/j.corsci.2015.11.005

[5] I. Salah, I.P. Parkin, E. Allan, Copper as an antimicrobial agent: recent advances, RSC Adv. **11**, 18179-18186 (2021). DOI: https://doi.org/10.1039/d1ra02149d

[6] M. Goudarzi, H. Ghaziasadi, The effect of gas flow rate on structural, mechanical and antibacterial properties of atmospheric plasma sprayed Cu coatings, Phys. Scr. **96**, 075601-075608 (2021). DOI: https://doi.org/10.1088/1402-4896/abf7fc

[7] G. Kear, B.D. Barker, F.C. Walsh, Electrochemical corrosion of unalloyed copper in chloride media-a critical review. Corr. Sci. **46**, 109-135 (2004). DOI: https://doi.org/10.1016/S0010-938X(02)00257-3

[8] F. Zucchi, V. Grassi, A. Frignani, G. Trabanelli, Inhibition of copper corrosion by silane coatings, Corr. Sci. **46**, 2853-2865 (2004). DOI: https://doi.org/10.1016/j.corsci.2004.03.019

[9] S. Patil, S.R. Sainkar, P.P. Patil, Poly(o-anisidine) coatings on copper: synthesis, characterization and evaluation of corrosion protection performance, Appl. Surf. Sci. **225**, 204-216 (2004). DOI: https://doi.org/10.1016/j.apsusc.2003.10.050

[10] A.V. Rao, S.S. Latthe, S.A. Mahadik, C. Kappenstein, Mechanically stable and corrosion resistant superhydrophobic sol-gel coatings on copper substrate, Appl. Surf. Sci. **257**, 5772-5776 (2011). DOI: ttps://doi.org/10.1016/j.apsusc.2011.01.099

[11] Y. Arafat, S.T. Sultana, I. Dutta, R. Panat, Effect of additives on the microstructure of electroplated Tin films, J. Electrochem. Soc. 165, D816-D824 (2018). DOI: https://doi.org/10.1149/2.0801816jes

[12] Z.X. Liu, S. Tian, Q. Li, J.C. Wang, J.B. Pu, G. Wang, W.J. Zhao, F. Feng, J. Qin, L.C. Ren, Integrated dual-functional ORMOSIL coatings with AgNPs@rGO nanocomposite for corrosion resistance and antifouling applications, ACS Sustainable Chem. Eng. **8**, 6786-6797 (2020). DOI: https://doi.org/10.1021/acssuschemeng.0c01294

[13] V.I.Chukwuike, R.S. Prasannakumar, K. Gnanasekar, R.C. Barik, Copper corrosion mitigation: A new insight for fabricating a surface barrier film against chloride ion under hydrodynamic flow, Appl. Surf. Sci. **555**, 149703-149718 (2021). DOI: https://doi.org/10.1016/j.apsusc.2021.149703

[14] S. Neupane, P. Losada-Pérez, U. Tiringer, P. Taheri, D. Desta, C.Y. Xie, D. Crespo, A. Mol, I. Milošev, A. Kokalj, F.U. Renner, Study of ercaptobenzimidazoles as inhibitors for copper, J. Electrochem. Soc. **168**, 051504-051516 (2021). DOI: https://doi.org/10.1149/1945-7111/abf9c3

[15] D.K. Kozlica, A. Kokalj, I. Milošev, Synergistic effect of 2-mercaptobenzimi- dazole and octylphosphonic acid as corrosion inhibitors for copper and aluminium – An electrochemical, XPS, FTIR and DFT study, Corr. Sci. **182**, 109082 (2021). DOI: https://doi.org/10.1016/j.corsci.2020.109082

[16] P. Durainatarajan, M. Prabakaran, S. Ramesh, Self-assembled monolayers of novel imidazole derivative on copper surface for anticorrosion protection in neutral medium, J. Adhesion Sci. Techn. **35**, 1895571-1895593 (2021). DOI: https://doi.org/10.1080/01694243.2021.1895571

[17] F.B. Ma, W.H. Li, H.W. Tian, B.R. Hou, The use of a new thiadiazole derivative as a highly efficient and durable copper inhibitor in 3.5% NaCl solution [J], Int. J. Electrochem. Sci. **105**, 862-5879 (2015).

[18] D. Gelman, D. Starovetsky, Y. Ein-Eli, Copper corrosion mitigation by binary inhibitor compositions of potassium sorbate and benzotriazole, Corr. Sci. **82**. 271-279 (2014). DOI: http://dx.doi.org/10.1016/j.corsci.2014.01.028

[19] A. Frignani, L. Tommesani, G. Brunoro, C. Monticelli, M. Fogagnolo, Influence of the alkyl chain on the protective effects of 1, 2, 3-benzotriazole towards copper corrosion.: Part I: inhibition of the anodic and cathodic reactions, Corr. Sci. **41**, 1205-1215 (1999). DOI: https://doi.org/10.1016/S0010-938X(98)00192-9

[20] S. Mamas, T. Kıyak, M. Kabasakaloglu, A. Koc, The effect of benzotriazole on brass corrosion, Mater. Chem. Phys. **93**, 41-47 (2005). DOI: https://doi.org/10.1016/j.matchemphys.2005.02.012

[21] P. Yu, D.M. Liao, Y.B. Luo, Z.G. Chen, Studies of benzotriazole and tolytriazole as inhibitors for copper corrosion in deionized water, Corrosion **59**, 314-318 (2003). DOI: https://doi.org/10.5006/1.3277563

[22] H.C. Kim, M.J. Kim, T. Lim, K.J. Park, K.H. Kim, S. Choe, S. Kim, J.J. Kim, Effects of nitrogen atoms of benzotriazole and its derivatives on the properties of electrodeposited Cu films, Thin Solid Films. **550**, 421-427 (2014). DOI: https://doi.org/10.1016/j.tsf.2013.10.124

[23] Y. Ein-Eli, E. Abelev, D. Starosvetsky, Electrochemical aspects of copper chemical mechanical planarization (CMP) in peroxide based slurries containing BTA and glycine, Electrochim. Acta. **49**, 1499-1503 (2004). DOI: https://doi.org/10.1016/j.electacta.2003.11.010

[24] F. Grillo, D.W. Tee, S.M. Francis, H.A. Früchtl, N.V. Richardson, Passivation of copper: Benzotriazole films on Cu(111), J. Phys. Chem. C **118**, 8667-8675 (2014). DOI: https://doi.org/10.1021/jp411482e

[25] D.Q. Zhang, L.X. Gao, G.D. Zhou, Synergistic effect of 2-mercapto benzimidazole and KI on copper corrosion inhibition in aerated sulfuric acid solution, J. Appl. Electrochem. **33**, 361-366 (2003). DOI: https://doi.org/10.1023/A:1024403314993

[26] A. Mezzi, E. Angelini, T.D. Caro, S. Grassini, F. Faraldi, C. Riccucci, G.M. Ingo, Investigation of the benzotriazole inhibition mechanism of bronze disease, Surf. Interface Anal. **44**, 968-971 (2012). DOI: https://doi.org/10.1002/sia.4841

[27] Z. Chen, L. Huang, G. Zhang, Y. Qiu, X. Guo, Benzotriazole as a volatile corrosion inhibitor during the early stage of copper corrosion under adsorbed thin electrolyte layers, Corr. Sci. **65**, 214-222 (2012). DOI: https://doi.org/10.1016/j.corsci.2012.08.019

[28] M.A. Deyab, Egyptian licorice extract as a green corrosion inhibitor for copper in hydrochloric acid solution, J. Ind. Eng. Chem. **22**, 384-389 (2015). DOI: https://doi.org/10.1016/j.jiec.2014.07.036

[29] H. Rahmani, E.I. Meletis, Corrosion inhibition of brazing Cu-Ag alloy with 1,2,3-benzotriazole and 2,5-dimercapto-1,3,4-thiadiazole, Corrosion **77**, 29-39 (2021). DOI: https://doi.org/10.5006/3642

[30] M. Soltani, T.J. Ravine, J.H. Davis, Novel boronium salt exhibits substantial antibacterial activity when compared to a commercial quaternary ammonium disinfectant, Bioorg. Med. Chem. Lett. **36**, 127808-127813 (2021). DOI: https://doi.org/10.1016/j.bmcl.2021.127808

[31] F.Y. Dong, T.S. Jia, Q. Wang, Y. Liu, L.X. Ma, S.J. Li, X.D. Tang, S.Y. Feng, Preparation of intrinsic antibacterial silicone rubber with matrix tethering quaternary ammonium salt groups, Mater. Today Commun. **26**, 101695-1017001 (2021).
DOI: https://doi.org/10.1016/j.mtcomm.2020.101695

[32] M.A. Hegazy, Ahmed Abdel Nazeer, K. Shalabi, Electrochemical studies on the inhibition behavior of copper corrosion in pickling acid using quaternary ammonium salts, J. Mol. Liq. **209**, 419-427 (2015). DOI: http://dx.doi.org/10.1016/j.molliq.2015.05.043

[33] X.M. Wang, Q. Wang, Y. Wan, Y. Ma, Inhibition Effect of Water-Soluble Chitosan N-quaternary Ammonium Salt on Carbon Steel in 0.25 M H_2SO_4 Solution, Int. J. Electrochem. Sci. **11**, 6229-6243 (2016). DOI: https://doi.org/10.20964/2016.07.10

[34] F. Rossi, C. Mele, M. Boniardi, B. Bozzini, Electrodeposition of Zn from alkaline electrolytes containing quaternary ammonium salts and ionomers: the impact of cathodic-anodic cycling conditions, ChemElectroChem. 1752-1764 (2020).
DOI: https://doi.org/10.1002/celc.202000165

[35] H.P. Lee, K. Nobe, Kinetics and mechanisms of Cu electrodissolution in chloride media, J. Electrochem. Soc. **133**, 2035-2043 (1986). DOI: https://doi.org/10.1002/chin.198705020

[36] Y. Qiang, H. Li, X. Lan, Self-assembling anchored film basing on two tetrazole derivatives for application to protect copper in sulfuric acid environment, J. Mater. Sci. Technol. **52**, 63-71 (2020).

[37] W. Chen. S. Hong, H.B. Li, H.Q. Luo, M. Li, N.B. Li, Protection of copper corrosion in 0.5 M NaCl solution by modification of 5-mercapto-3-phenyl-1,2,4-thiadiazole-2-thione potassium self-assembled monolayer, Corros. Sci. **61**, 53-62 (2012).
DOI: https://doi.org/10.1016/j.corsci.2012.04.023

[38] F.T. Li, Z.K. Wang, Y.Y. Jiang, C.L. Li, S.Q. Sun, S.G. Chen, S.Q. H, DFT study on the adsorption of deprotonated benzotriazole on the defective copper surfaces, Corr. Sci. **186**, 109458-109471 (2021). DOI: https://doi.org/10.1016/j.corsci.2021.109458

[39] X.L. Zuo, W.P. Li, W. Luo, X.Z. Zhang, Y.J. Qiang, J. Zhang, H. Li, B.C. Tan, Research of Lilium brownii leaves extract as a commendable and green inhibitor for X70 steel corrosion in hydrochloric acid, J. Molecular Liquids. **321**, 114914-114923 (2021). DOI: https://doi.org/10.1016/j.molliq.2020.114914

[40] A.K. Satapathy, G. Gunasekaran, S.C. Sahoo, K. Amit, P.V. Rodrigues, Corrosion inhibition by Justicia gendarussa plant extract in hydrochloric acid solution, Corr. Sci. **51**, 2848-2856 (2009). DOI: https://doi.org/10.1016/j.corsci.2009.08.016

[41] F.B. Rowcock, R.J. Jasinski, Time-resolved impedance spectroscopy of mild steel in concentrated hydrochloric acid, J Electrochem Soc. **136**, 2310-2314. (1989).

[42] Matjazˇ Finšgar, Ingrid Milošev, Inhibition of copper corrosion by 1,2,3-benzotriazole: A review, Corr. Sci. **52**, 2737-2749 (2010). DOI: https://doi.org/10.1016/j.corsci.2010.05.002.

[43] H. Rahmani, E.I. Meletis, Corrosion study of brazing Cu-Ag alloy in the presence of benzotriazole inhibitor. Applied Surf. Sci. **497**, 143759-143766 (2019).
DOI: https://doi.org/10.1016/j.apsusc.2019.143759

[44] C. Jing, Z. Wang, Y. Gong, H. Huang, Y. Ma, H. Xie, H.Li, S. Zhang, F. Gao, Photo and thermally stable branched corrosion inhibitors containing two benzotriazole groups for copper in 3.5 wt% sodium chloride solution, Corr. Sci, **138**, 353-371 (2018). DOI: https://doi.org/10.1016/j.corsci. 2018.04.027

[45] M. Yadav, R.R. Sinha, S. Kamar, T.K, Sarkar, Corrosion inhibition effect of spiropyrimidinethiones on mild steel in 15% HCl solution: insight from electrochemical and quantum studies. RSC. Adv. **5**, 70832-70848 (2015).
DOI: https://doi.org/10.1039/c5ra14406j

[46] P. Arellanes-Lozada, O. Olivares-Xometl, N.V. Likhanova, I.V. Lijanova, J.R. Vargas-Garcia, R.E. Hernandez-Ramirez, Adsorption and performace of ammonium-base ionic liquid as corrosion inhibitors of steel, J. Mol. Liq. **265**, 151-163 (2018).
DOI: https://doi.org/10.1016/j.molliq. 2018.04.153

[47] J. Wang, Z. Wei, S. Mao, H. Li, Y. Wang, Highly uniform Ru nanoparticles over N-doped carbon: pH and temperature-universal hydrogen release from water reduction. Energy Environ. Sci. **11**, 800-806 (2018). DOI: https://doi.org/10.1039/C7EE03345A

[48] J.B. Lhoest, S. Bartiaux, P.A. Gerin, M.J. Genet, P. Berfrand, P.G. Rouxhet, Poly(amion acids) by XPS: analysis of poly-L-Leucine, Surf. Sci. Spectra **3,** 348-356 (1994).
DOI: https://doi.org/10.1116/1.1247787

[49] I. Carrillo, E. Sanchez de la Blance, J.L.G. Fierro, M.A. Raso, F. Accion, E. Enciso, M.I. Redondo, Conductivity and long term stability of polypyrrole poly(styrene-co-methacrylic acid) core-shell particles at different polypyrrole loadings, Thin Solid Films. **539**, 154-160. (2013).
DOI: https://doi.org/10.1016/j.tsf.2013.05.086

[50] Y.E. Jo, D.Y. Yu, S.K. Cho, Revealing the inhibition effect of quaternary ammonium cations on Cu electrodeposition, J. Appl. Electrochem. **50**, 245-253 (2020).
DOI: https://doi.org/10.1007/s10800-019-01381-4